

Effect of Strain Rate on the Bainitic Transformation in Fe-C-Mn-Si Medium-Carbon Bainitic Steels



GUANGHUI CHEN, GUANG XU, HATEM S. ZUROB, HAIJIANG HU,
and XIANGLIANG WAN

The effect of strain rate on the kinetics of the bainitic transformation in a Fe-C-Mn-Si medium-carbon bainitic steel was investigated by dilatometry, metallography, and X-ray diffraction. The results indicate that the bainitic transformation is affected by the strain rate. The bainitic transformation is significantly promoted by deformation at a low strain rate of 0.01 s^{-1} , and the amount of bainite increases further when the strain rate increases to 0.1 s^{-1} . However, as the strain rate increases further to 1.0 and 5.0 s^{-1} , the extent to which deformation promotes the bainitic transformation decreases, and the amount of bainitic transformation is smaller than that at low strain rates. The amount of bainite tends to be constant with increasing strain rate from 1.0 to 5.0 s^{-1} . In addition, the volume fraction of retained austenite shows the same trend as the amount of bainite, indicating that chemical stabilization plays a key role in determining the amount of retained austenite. Moreover, the strain rate has no significant effect on the bainite morphology.

<https://doi.org/10.1007/s11661-018-5051-z>

© The Minerals, Metals & Materials Society and ASM International 2018

I. INTRODUCTION

THE development of advanced high-strength steels is attracting increasing attention. The interest in bainitic steels is due to their excellent mechanical properties.^[1–3] Bhadeshia and Caballero reported a novel bainite steel with a strength of 2.5 GPa .^[4–6] It is generally accepted that ausforming leads to accelerated nucleation and retarded bainite growth.^[7] Defects such as dislocations induced by deformation can enhance the nucleation rate and shorten the incubation time of the bainitic transformation.^[8,9] However, excess deformation constrains bainite growth and results in finer microstructure.^[10,11] In addition, the size of undercooled austenite grains decreases owing to deformation, which limits the growth of bainite.

Many researchers^[7,12–17] have investigated the effect of different strain levels and deformation temperatures on the bainitic transformation. Hu^[7,12] found that deformation at high temperature ($860 \text{ }^\circ\text{C}$) retards the

bainitic transformation in Fe-C-Mn-Si bainitic steels, whereas small strains at low temperature (300 to $400 \text{ }^\circ\text{C}$) promote the bainitic transformation. The extent to which deformation promotes the transformation decreases with increasing strain and temperature. Gong^[15] investigated the effect of ausforming on the bainitic transformation and claimed that deformation at $600 \text{ }^\circ\text{C}$ has little influence on the bainitic transformation and that deformation at $300 \text{ }^\circ\text{C}$ promotes the bainitic transformation. Fan^[16] reported that strain at 600 to $700 \text{ }^\circ\text{C}$ retards the bainitic transformation, whereas strain at $300 \text{ }^\circ\text{C}$ not only promotes the bainitic transformation but also refines bainite ferrite; Chiou *et al.*^[18] reported similar results. In addition, Zhou^[19,20] investigated the effect of a combination of strain and stress on the bainitic transformation and concluded that stress can further promote the bainitic transformation.

Therefore, there have been many investigations on the effects of strain, temperature, and even stress on the transformation of high-strength bainitic steels in the last decade. Further, some studies have investigated the effect of strain rate on the ferrite transformation. For example, Zhou *et al.*^[21] and Tian *et al.*^[22] studied the effect of strain rate on ferrite precipitation and claimed that the extent of promotion was reduced by increasing the strain rate. However, there is no report on the effect of strain rate on the transformation of high-strength bainitic steels. Deformation parameters such as the strain amount, temperature, and strain rate inevitably affect the bainitic transformation because these parameters affect the defect density and distortion energy of

GUANGHUI CHEN, GUANG XU, HAIJIANG HU, and XIANGLIANG WAN are with the The State Key Laboratory of Refractories and Metallurgy, Hubei Collaborative Innovation Center for Advanced Steels, Wuhan University of Science and Technology, Wuhan 430081, China. Contact e-mail: xuguang@wust.edu.cn HATEM S. ZUROB is with the Department of Materials Science and Engineering, McMaster University, 1280 Main St. W., Hamilton L8S4L7, Canada.

Manuscript submitted July 11, 2018.

Article published online November 29, 2018

the deformed microstructure. Thus, the microstructure and properties of bainitic steels will be affected by the strain rate. If deformation at a certain strain rate can promote the bainitic transformation, then this strain rate can be applied in the processing of bainitic steels to obtain the maximum amount of bainite in the microstructure. Therefore, the effect of strain rate on the bainitic transformation of high-strength bainitic steels should be clarified and a theoretical reference should be provided for determining appropriate processing technology for high-strength bainitic steels.

II. EXPERIMENTAL PROCEDURES

The experimental steel is a Fe-0.36C-2.8Mn-1.8Si (wt pct) high-strength bainitic steel. High-carbon bainitic steels possess ultrahigh strength, but it takes a long time to complete the bainitic transformation. Therefore, a medium carbon content of 0.36 wt pct was added to the tested steel to shorten the bainitic transformation. Manganese at 2.8 wt pct was used because manganese is a strengthening element and facilitates bainite formation by increasing the hardenability. In addition, silicon can suppress the formation of cementite, and 1.8 wt pct silicon was added to obtain carbide-free bainite. The steel was refined and cast in the form of 50 kg ingots using a laboratory-scale vacuum furnace. The resulting ingots were hot-rolled to 14-mm-thick plates and air-cooled to room temperature. The specimens for the thermomechanical simulation tests were machined in the form of cylinders 6.0 mm in diameter and 10.0 mm in height.

Thermal simulation experiments were conducted on a Gleeble 3500 simulator. Figure 1 shows the experimental procedures. The specimens were first heated to 1000 °C at 5 °C/s and held for 15 minutes. Then, the specimens were cooled to 400 °C at 20 °C/s. This cooling rate was fast enough to avoid ferrite and pearlite formation.^[7,12] All specimens were held for 10 seconds at 400 °C to eliminate thermal gradients before compression. The austenitized specimens were deformed at 400 °C to a strain of 0.3 at strain rates of 5.0, 1.0, 0.1, and 0.01 s⁻¹. The deformed specimens were held at 400 °C for 15 minutes to observe the bainitic

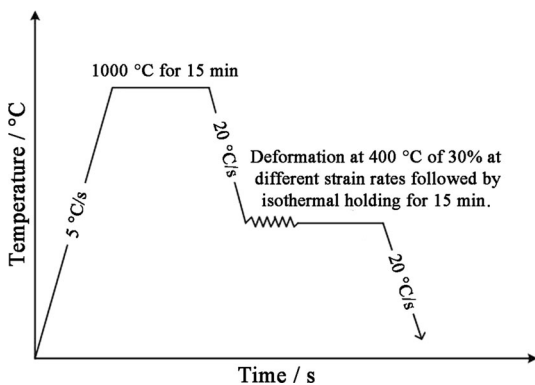


Fig. 1—Experimental procedures for thermal simulation experiments.

transformation. Finally, the specimens were cooled to room temperature at 20 °C/s. A specimen without deformation was heat-treated for comparison. In all cases, the diameter of the specimens (degree of dilatation) during the isothermal bainitic transformation was recorded by a thermal dilatometer installed in the simulator.

All the specimens were polished and etched with 4 pct nital, and their microstructure were observed at room temperature by field emission scanning electron microscopy (FE-SEM; Nova 400 Nano) at an acceleration voltage of 18 kV. The volume fraction of retained austenite (RA) in each specimen was determined using X-ray diffraction (XRD; X'Pert) with Co K α radiation under the following conditions: acceleration voltage, 40 kV; current, 150 mA; step size, 0.06 deg. The calculation of the RA is based on the integrated intensities of the (200) α , (211) α , (200) γ , (220) γ , and (311) γ diffraction peaks.

III. RESULTS

A. Dilatation

After thermal simulation experiments, the deformed specimens were compressed to the shape of a drum. The changes in the middle diameter of the specimens were recorded as the dilatation. The microstructure in the middle section of the specimens was observed. The diameter of each specimen in the thermal simulation experiment was recorded during the entire heat treatment process. Figure 2 shows the dilatation of the specimen deformed at a strain rate of 1.0 s⁻¹. The specimen was heated to 1000 °C (before point A) and held for 15 minutes (from point A to B), followed by cooling to 400 °C (from point B to C). Next, the specimen was deformed at 1.0 s⁻¹. The sudden increase in diameter from point C to point D is due to the applied deformation. When the stress was released, the diameter of the specimen decreased because the elastic deformation was eliminated (from point D to point E). After

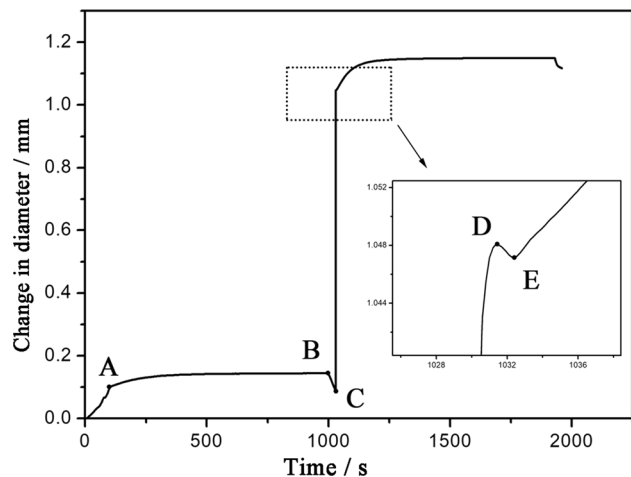


Fig. 2—Dilatation changes with time during deformation of specimen deformed at 1.0 s⁻¹.

point E, the bainitic transformation occurred, and the dilatation increased again. Finally, the diameter of the specimen tended to be constant, indicating that the bainitic transformation was complete. Note that the heat caused by deformation, especially at higher strain rates such as 1.0 and 5.0 s⁻¹, would affect the transformation temperature. This might influence the dilatation signal. In addition, the thermal contraction during cooling to 400 °C could also distort the dilatation signal. To examine this potential problem, the temperature curve of the specimen deformed at 5.0 s⁻¹ during thermal holding at 400 °C is shown in Figure 3; it shows a constant temperature of 400 °C. Therefore, the dilatation signal was not affected by deformation heating and thermal contraction.

The dilatation results suggest that a very small amount of bainitic transformation is unavoidable during the cooling process from the austenitization temperature to 400 °C. Some bainite could even form during deformation. The evaluation of the bainitic transformation kinetics was begun at point E, after deformation. From point C to point E, compressive deformation and elastic recovery occurred. For strain rates of 0.01, 0.1, 1.0, and 5.0 s⁻¹, the time was 35.90, 3.69, 2.28, and 2.25 seconds, respectively. Note that the bainitic transformation might occur during deformation at a low strain rate of 0.01 s⁻¹. According to the authors' previous study,^[23] the amount of bainitic transformation during deformation of medium-carbon steel was very small. Therefore, the amount of bainitic transformation can be ignored. In addition, the diameter of the specimen affects the dilatation amount at the same amount of bainitic transformation. The dilatation increases with increasing diameter of the specimen. To compare the dilatation under different conditions, the dilatation amount of different specimens was normalized using the formula $(d_i - d_0)/D_0$, where d_i is the instantaneous diameter during isothermal holding, d_0 is the initial diameter (point E), and D_0 is the diameter corresponding to the starting point of thermal holding at 400 °C after deformation.^[12] Figures 4(a) and (b) show the change in the normalized dilatation during

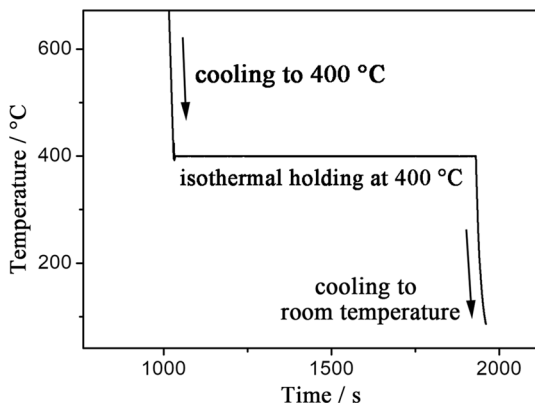


Fig. 3—Temperature curve of the specimen deformed at 5.0 s⁻¹ during thermal holding at 400 °C.

isothermal holding under different deformation conditions. The dilatation changes in Figures 4(a) and (b) represent the amount of bainitic transformation during isothermal holding at 400 °C because the variation in the specimen diameter (dilatation) is caused by the bainitic transformation. The bainitic transformation is obviously promoted by deformation ($\epsilon = 0.3$), which is consistent with previous works.^[7,12–17]

Figure 4(c) shows the relationship between the normalized final dilatation and strain rate for the experimental steel. Note that the amount of bainitic transformation first increases, then decreases with increasing strain rate, and finally tends to be constant. The maximum amount of bainitic transformation appears at a strain rate of 0.1 s⁻¹. This demonstrates that the effect of deformation on the bainitic transformation varies with the strain rate. In addition, the final amount of bainite in the undeformed specimen is significantly lower than that in the deformed steels. The transformation time for the specimen without deformation is 90 minutes.

B. Microstructure

To determine the volume fractions of bainite in all the specimens from SEM images, Image-Pro Plus software was used to calculate the proportions of each type of microstructure. Figure 5 presents an example (the specimen deformed at 0.1 s⁻¹) to illustrate the method. According to the calculation procedure in the authors' previous study,^[24] the bainite volume fraction for the undeformed specimen is 8.95 pct, and those for specimens deformed at 0.01, 0.1, 1.0, and 5.0 s⁻¹ are 49.90 pct, 53.94 pct, 41.82 pct, and 42.36 pct, respectively. The results obtained by quantitative microscopy analysis are consistent with the dilatometry results.

The SEM images in Figure 6 show the microstructure of the specimens. Only a small amount of needle-like bainite (labeled B) appears in the undeformed specimen. There is clearly more bainite in the deformed specimens than in the undeformed specimen (Figures 6(d) and (e)). Compared with that in the undeformed specimen, the bainite in the deformed specimens tends to be thinner and shorter owing to deformation. Moreover, the specimen deformed at 0.1 s⁻¹ contains the largest amount of bainite (Figure 6(c)) among all the specimens. In addition, the amount of bainite in the specimens deformed at 1.0 and 5.0 s⁻¹ is similar (Figures 6(d) and (e)). The microstructure is consistent with the dilatation results in Figure 4. In addition, all the specimens contain martensite (labeled M) in lightly etched areas. The bainitic transformation is characterized by incomplete transformation.^[25,26] During the cooling process, much of the untransformed austenite is transformed to martensite.

C. Retained Austenite

Figure 7 shows the diffraction patterns of the undeformed and deformed specimens. The fraction of RA in each specimen can be calculated using formula (1)^[26]:

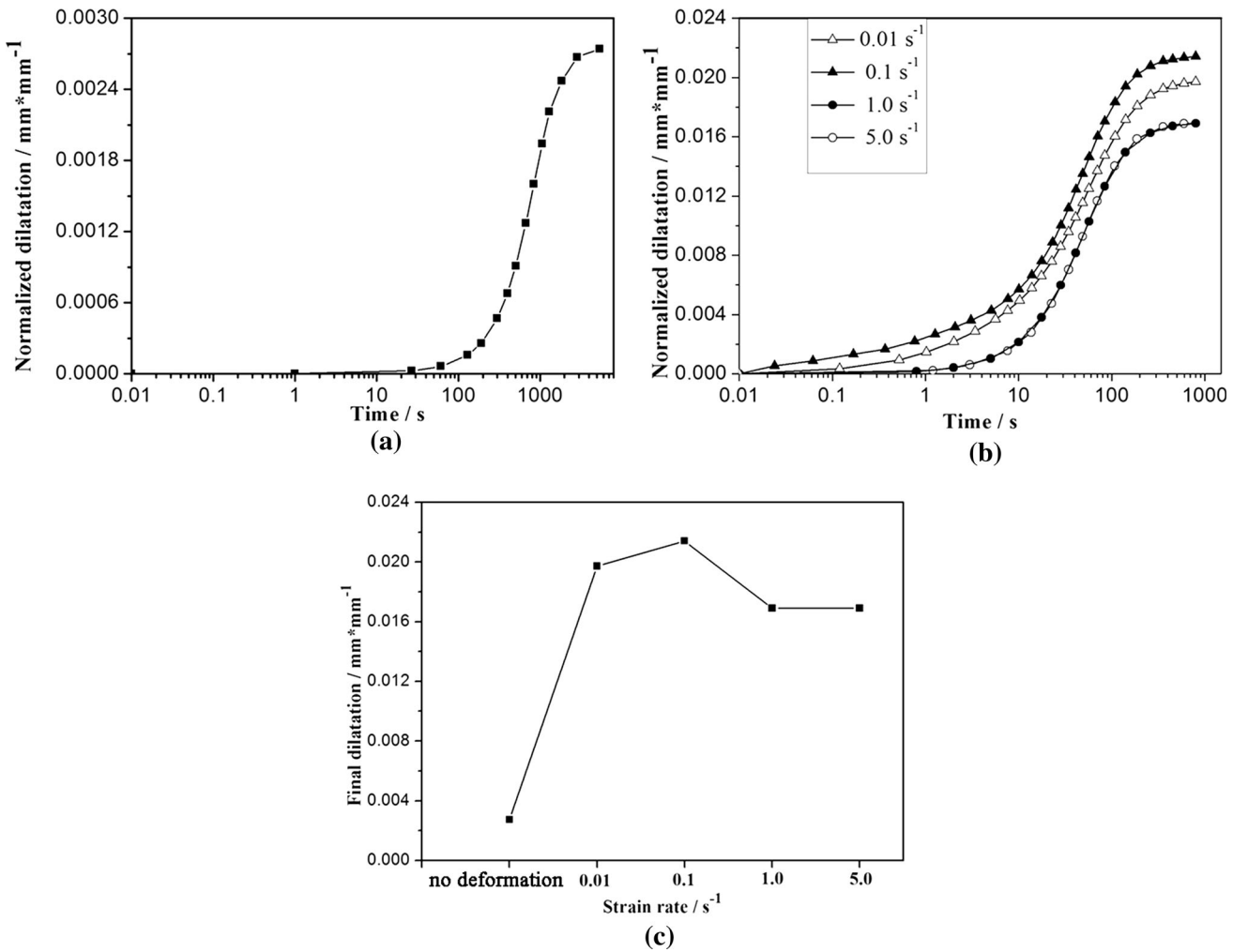


Fig. 4—(a) Normalized dilatation changes of undeformed specimen held at 400 °C for 90 min on logarithmic scale, (b) normalized dilatation changes after deformation of deformed specimens on logarithmic scale, (c) normalized final dilatation representing the amount of bainitic transformation during isothermal holding.

$$V_i = \frac{1}{1 + G(I_\alpha/I_\gamma)}, \quad [1]$$

where V_i is the volume fraction of austenite for each peak, and I_α and I_γ are the integrated intensities of the ferrite and austenite peaks, respectively. The following G values for each peak were used: 2.5 for $I_{\alpha(200)}/I_{\gamma(200)}$, 1.38 for $I_{\alpha(200)}/I_{\gamma(220)}$, 2.02 for $I_{\alpha(200)}/I_{\gamma(311)}$, 1.19 for $I_{\alpha(211)}/I_{\gamma(200)}$, 0.06 for $I_{\alpha(211)}/I_{\gamma(220)}$, and 0.96 for $I_{\alpha(211)}/I_{\gamma(311)}$.^[27] The carbon content was calculated using formula (2):

$$X_C = V_\gamma \times X_{Cin\gamma} + V_\alpha \times X_{Cin\alpha}, \quad [2]$$

where X_C is the original carbon content of the experimental steel (0.36 wt pct). V_γ is the fraction of untransformed austenite after isothermal holding, which includes the RA and martensite; the value of V_γ can be taken as $1 - V_\alpha$. $X_{Cin\gamma}$ represents the carbon content of the untransformed austenite, which can represent the carbon content of the RA^[28]; V_α is the calculated fraction of bainite ferrite according to the SEM

micrograph; and $X_{Cin\alpha}$ is the theoretical carbon content of the α phases, which is very low and is regarded as zero.^[28] Thus, the carbon content of the RA is calculated as 0.395 wt pct for the undeformed specimen. The theoretical values of the carbon content of the RA in the specimens deformed at 0.01, 0.1, 1.0, and 5.0 s⁻¹ are 0.719, 0.782, 0.619, and 0.625 wt pct, respectively. The RA fraction in the undeformed specimen is only approximately 7.79 pct, which is significantly lower than those in the deformed specimens. The amount of RA is determined by mechanical and chemical stabilization. Deformation causes mechanical stabilization, which contributes to the increase in RA. Chemical stabilization also affects the amount of RA. The chemical stabilization of austenite in the deformed specimens increases owing to the formation of a larger amount of bainite. Moreover, the amount of RA increases with strain rate up to 0.1 s⁻¹ and then decreases as the strain rate increases. Note that the maximum amount of RA appears at a strain rate of 0.1 s⁻¹, which corresponds to the maximum amount of bainite.

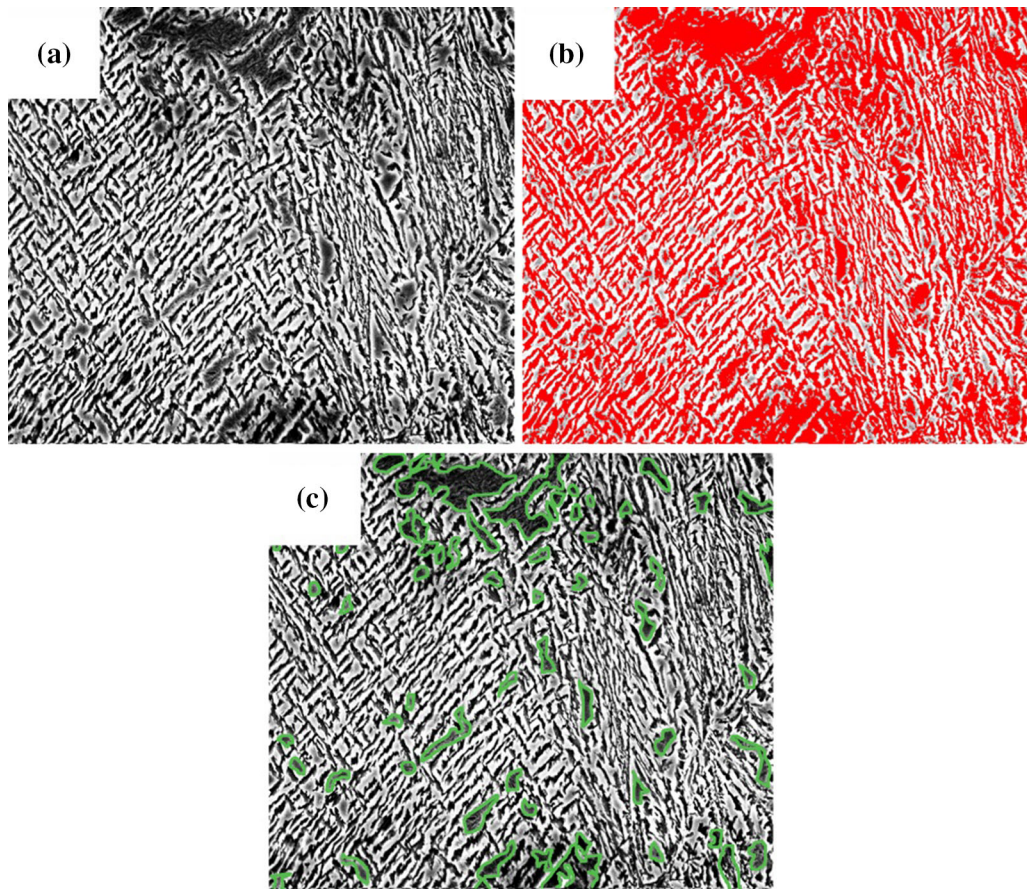


Fig. 5—Example (for specimen deformed at 0.1 s^{-1}) illustrating the method of determining the volume fraction of bainite: (a) the original micrograph, (b) the darker area consisting of bainite and martensite/austenite (M/A) is colored red, (c) the blocky darker area consisting of M/A is marked with green lines (Color figure online).

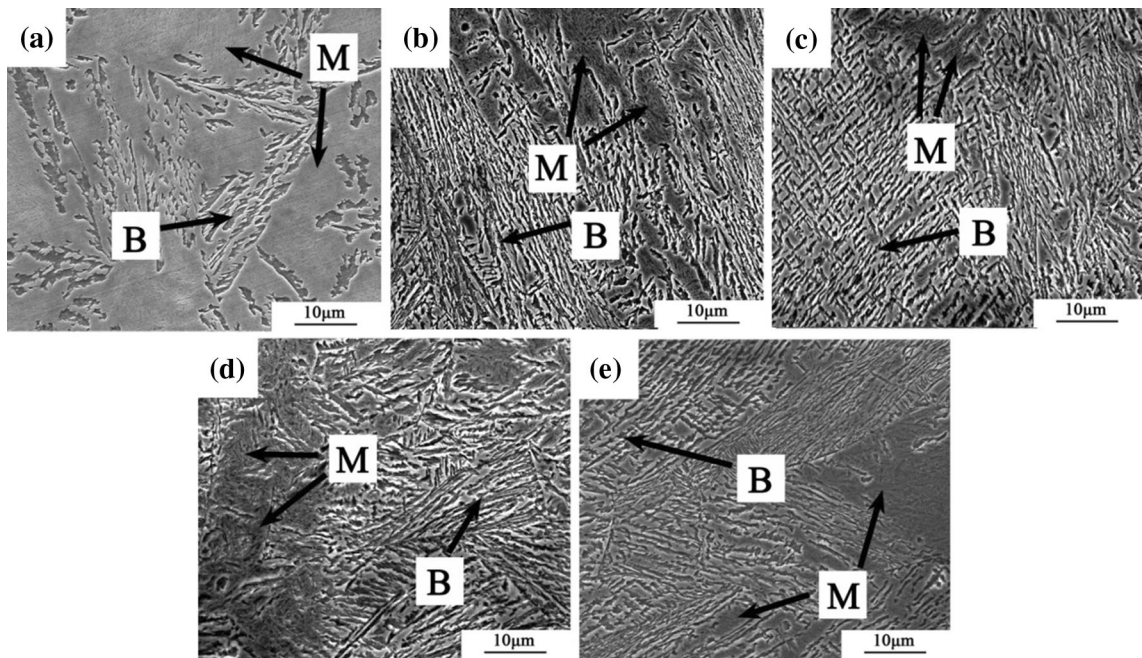


Fig. 6—SEM microstructure: (a) no deformation + $400 \text{ }^\circ\text{C}$ for 90 min; deformation at (b) 0.01 s^{-1} , (c) 0.1 s^{-1} , (d) 1.0 s^{-1} , and (e) 5.0 s^{-1} + 15 min.

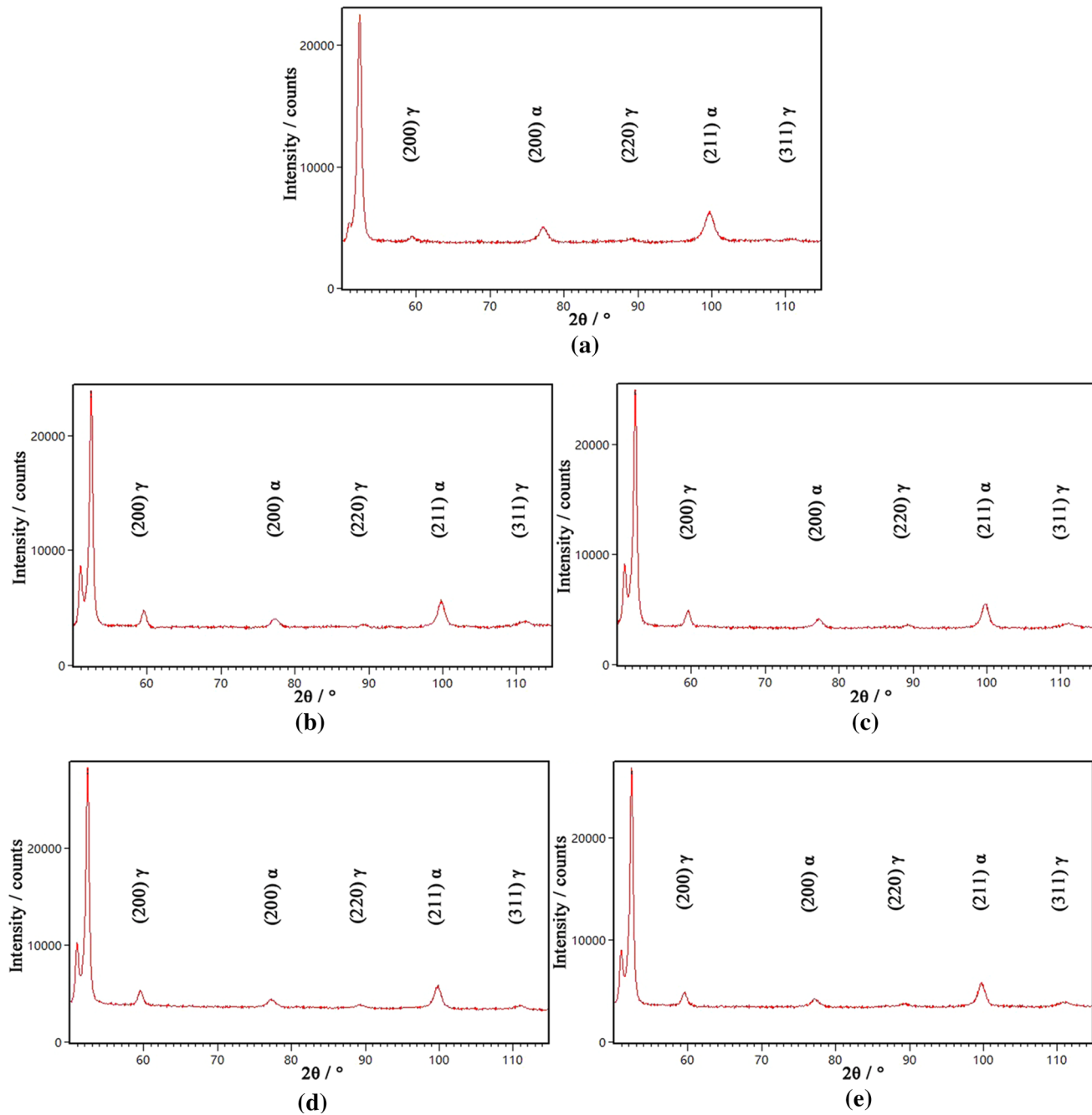


Fig. 7—Diffraction patterns of all specimens: (a) undeformed and deformed at (b) 0.01 s^{-1} , (c) 0.1 s^{-1} , (d) 1.0 s^{-1} , and (e) 5.0 s^{-1} .

IV. DISCUSSION

A. Bainitic Transformation

The bainitic transformation kinetics is affected by three factors: the incubation time, transformation velocity, and final transformed volume fraction. Deformation bands evidently provide heterogeneous nucleation sites and shorten the incubation time.^[7,11]

Figures 4(a) and (b) show that both the velocity and transformed volume fraction of bainite in the undeformed specimen are smaller than those in the deformed specimens. The chemical stabilization of austenite in the tested steel is enhanced because the austenite content

stabilizes elements such as C, Si, and Mn. Therefore, the bainitic transformation in the undeformed specimen is extremely slow. When the specimens are deformed to 30 pct strain at strain rates of 0.01 and 0.1 s^{-1} , the transformation velocity and amount of bainite increase greatly. When the specimen is deformed at 0.01 or 0.1 s^{-1} , the high dislocation density offers more heterogeneous nucleation sites for the bainitic transformation, resulting in an obvious increase in the bainitic transformation kinetics. On the other hand, the amount of bainitic transformation decreases when the strain rate increases to 1.0 and 5.0 s^{-1} compared with those of specimens deformed at 0.01 and 0.1 s^{-1} . This is

attributed to retardation of dislocations in bainite growth because of excess dislocations in the specimens deformed at 1.0 and 5.0 s⁻¹.^[13] However, the amount of bainitic transformation in specimens deformed at 1.0 and 5.0 s⁻¹ is still obviously larger than that in the undeformed specimen. Ausforming is known to have the dual effect of accelerating nucleation and retarding growth during the bainitic transformation.^[29] Deformation defects such as dislocations facilitate nucleation for the bainitic transformation but limit bainite growth. Dynamic recovery may occur during deformation.^[30] The dislocation density is higher in specimens at high strain rates because the dynamic recovery is reduced.^[31] This results in greater retardation of bainite growth. The competition between accelerated nucleation and retarded growth determines the effect of strain rate on the bainitic transformation.

Figure 6 indicates that the undeformed specimen contains the least bainite owing to chemical stabilization. The final amount of bainite in the deformed specimens is much larger than that in the undeformed specimen, and the bainite sheaves in the deformed specimens are obviously finer and shorter. Dislocations in austenite grains introduced by deformation retard the growth of bainite, leading to shorter and finer bainite plates. In addition, no recrystallization occurs during deformation.^[23] The austenite grain size after deformation depends mainly on the strain amount. Therefore, the bainite morphology in the deformed specimens does not change with the strain rate (Figures 6(b) through (e)).

B. Retained Austenite

Figures 4(c) and 8 indicate that as a function of strain rate, the RA content has the same trend as the bainite volume fraction. The final RA content depends on the chemical stabilization and mechanical stabilization of the residual austenite. The bainitic transformation is always accompanied by carbon rejection; i.e., carbon diffuses into the surrounding untransformed austenite.^[32] Thus, the increase in the amount of bainite due to deformation enhances the chemical stabilization of the

residual austenite. In addition, deformation boosts the mechanical stabilization of the residual austenite. As a result, the two factors lead to a higher C content in the untransformed austenite in the deformed specimens compared to that in the specimen without deformation. The carbon content in Figure 8 shows essentially the same trend as the amount of RA, suggesting that chemical stabilization by the carbon content plays a major role in determining the amount of RA.

The specimen deformed at 0.1 s⁻¹ contains more bainite, which results in a higher carbon content in the residual austenite and less martensite in the deformed specimens. On the other hand, the specimen deformed at 5.0 s⁻¹ has the least bainite, which leads to a decrease in the carbon content and chemical stabilization in the residual austenite. Subsequently, more martensite is transformed, and a lower amount of RA is retained. The amount of RA depends on the amount of bainitic transformation as well as the amount of martensitic transformation.

V. CONCLUSIONS

The effect of strain rate on the kinetics of the bainitic transformation in a Fe-C-Mn-Si medium-carbon bainitic steel was investigated. The following conclusions can be drawn:

- (1) The strain rate apparently affects the bainitic transformation in Fe-C-Mn-Si medium-carbon bainitic steels. The bainitic transformation is significantly promoted by deformation of austenite to 30 pct strain at various strain rates. The extent to which the transformation is promoted first increases with strain rate and then decreases, before finally tending to becoming independent of the strain rate.
- (2) The strain rate has no significant effect on the bainite morphology.
- (3) The amount of RA at a constant strain depends mainly on the chemical stabilization in this study.

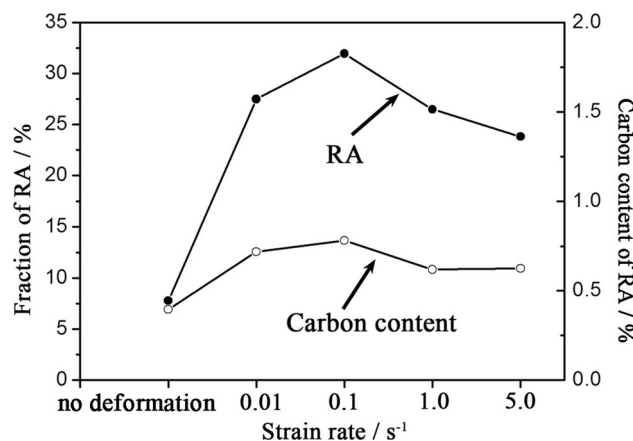


Fig. 8—Amount of RA and carbon content of RA for different specimens.

ACKNOWLEDGMENT

The authors gratefully acknowledge the financial supports from the National Natural Science Foundation of China (NSFC) (Nos. 51874216 and 51704217) and the Major Projects of Technology Innovation of Hubei Province (No. 2017AAA116).

REFERENCE

1. H.K. Sung, S.Y. Shin, B. Hwang, C.G. Lee, N.J. Kim, and S. Lee: *Metall. Mater. Trans. A*, 2011, vol. 42, pp. 1827–35.
2. S.H. He, B.B. He, K.Y. Zhu, and M.X. Huang: *Acta Mater.*, 2018, vol. 149, pp. 46–56.
3. A. Lambert-Perlade, T. Sturel, A.F. Gourgues, J. Besson, and A. Pineau: *Metall. Mater. Trans. A*, 2004, vol. 35, pp. 1039–53.

4. C. Garciamateo, F.G. Caballero, and H.K.D.H. Bhadeshia: *Mater. Sci. Forum.*, 2005, vol. 112, pp. 285–88.
5. F.G. Caballero, C. Garcia-Mateo, and M.K. Miller: *JOM*, 2014, vol. 66, pp. 747–55.
6. C. Garcia-Mateo, F.G. Caballero, T. Sourmail, M. Kuntz, J. Cornide, V. Smanio, and R. Elvira: *Mater. Sci. Eng. A*, 2012, vol. 549, pp. 185–92.
7. H.J. Hu, G. Xu, L. Wang, M.X. Zhou, and Z.L. Xue: *Met. Mater. Int.*, 2015, vol. 21, pp. 929–35.
8. J.G. He, A.M. Zhao, Y. Huang, C. Zhi, and F. Zhao: *Mater. Today.*, 2015, vol. 2, pp. 289–94.
9. B.B. He, W. Xu, and M.X. Huang: *Philos. Mag.*, 2015, vol. 95, pp. 1150–63.
10. R.H. Larn and J.R. Yang: *Mater. Sci. Eng. A*, 2000, vol. 278, pp. 278–91.
11. B.B. He, W. Xu, and M.X. Huang: *J. Mater. Sci. Technol.*, 2017, vol. 33, pp. 1494–1503.
12. H.J. Hu, G. Xu, L. Wang, and M.X. Zhou: *Steel. Res. Int.*, 2017, <https://doi.org/10.1002/srin.201600170>.
13. H.J. Hu, H.S. Zurob, G. Xu, D. Ernbury, and G.R. Purdy: *Mater. Sci. Eng. A*, 2015, vol. 626, pp. 34–40.
14. H.J. Hu, G. Xu, M.X. Zhou, and Q. Yuan: *Met. Mater. Inter.*, 2017, vol. 23, pp. 233–38.
15. W. Gong, Y. Tomota, Y. Adachi, A.M. Paradowska, J.F. Kelleher, and S.Y. Zhang: *Acta Mater.*, 2013, vol. 61, pp. 4142–54.
16. H.L. Fan, A.M. Zhao, Q.C. Li, H. Guo, and J.G. He: *Int. J. Miner. Metall. Mater.*, 2017, vol. 24, pp. 264–70.
17. J. Zhao, X. Jia, K. Guo, and T.S. Wang: *Mater. Sci. Eng. A*, 2017, vol. 682, pp. 527–34.
18. C.S. Chiou, J.R. Yang, and C.Y. Huang: *Mater. Chem. Phys.*, 2001, vol. 69, pp. 113–24.
19. M.X. Zhou, G. Xu, L. Wang, and H.J. Hu: *Met. Mater. Int.*, 2016, vol. 22, pp. 956–61.
20. M.X. Zhou, G. Xu, H.J. Hu, Q. Yuan, and J.Y. Tian: *Steel. Res. Int.*, 2017, <https://doi.org/10.1002/srin.201600377>.
21. R.F. Zhou, W.Y. Yang, Z.Q. Sun, and J.P. He: *Chin. J. Eng.*, 2004, vol. 26, pp. 512–18 (In Chinese).
22. J. Tian, W.Y. Yang, and Z.Q. Sun: *Trans. Mater. Heat. Treat.*, 2005, vol. 26, pp. 62–67 (In Chinese).
23. G.H. Chen, G. Xu, H.J. Hu, Q. Yuan, and Q.X. Zhang: *Steel. Res. Int.*, 2018, <https://doi.org/10.1002/srin.201800201>.
24. J.Y. Tian, G. Xu, M.X. Zhou, and H.J. Hu: *Steel. Res. Int.*, 2018, <https://doi.org/10.1002/srin.201700469>.
25. T. Furuhashi, T. Yamaguchi, G. Miyamoto, and T. Maki: *Met. Sci. J.*, 2010, vol. 26, pp. 392–97.
26. W.T. Reynolds, S.K. Liu, F.Z. Li, S. Hartfield, and H.I. Aaronson: *Metall. Trans. A*, 1990, vol. 21, pp. 1479–91.
27. S.B. Singh and H.K.D.H. Bhadeshia: *Mater. Sci. Eng. A*, 1998, vol. 245, pp. 72–79.
28. H.D. Wu, G. Miyamoto, Z.G. Yang, C. Zhang, H. Chen, and T. Furuhashi: *Acta Mater.*, 2017, vol. 133, pp. 1–9.
29. M. Kabirmohammadi, B. Avishan, and S. Yazdani: *Mater. Chem. Phys.*, 2016, vol. 184, pp. 306–17.
30. H.T. Liu, W. Meng, G. Fei, and Z.Y. Liu: *J. Northeast. Univ.*, 2012, vol. 33, pp. 1734–36.
31. W.S. Lee and C.W. Chen: *Mater. Sci. Eng. A*, 2013, vol. 576, pp. 91–100.
32. Y. Sakuma, O. Matsumura, and H. Takechi: *Metall. Trans. A*, 1991, vol. 22, pp. 489–98.